Interaction of prion peptide PrP 180-193 with DPPC model membranes: a thermodynamic study

D. Grasso,*[a] D. Milardi,[b] V. Guantieri,[c] C. La Rosa[a] and E. Rizzarelli[ab]

[a] *Dipartimento di Scienze Chimiche, Università di Catania, Viale Andrea Doria 6, 95125, Catania, Italy. E-mail: dgrasso@dipchi.unict.it; Fax: ++39 (0) 95 580138; Tel: ++ (0) 95 7385204*
[b] *Istituto di Biostrutture e Bioimmagini CNR - Sezione di Catania, Viale Andrea Doria 6, 95125, Catania, Italy*
[c] *Dipartimento di Chimica Inorganica, Metallorganica ed Analitica, Università di Padova, Via F. Marzolo 1, 35131, Padova, Italy*

Received (in London, UK) 22nd October 2002, Accepted 29th November 2002
First published as an Advance Article on the web 2nd January 2003

The conversion of Prion (PrP^c), a protein normally found on the outer surface of neurons, into an abnormal conformer (PrP^{sc}) is a key molecular event in the pathogenesis of Prion diseases. Recent experimental observations support the hypothesis that an abnormal interaction of PrP with the lipid membrane might be involved in the conversion of PrP^c into PrP^{sc}. Particularly, a peptide with an amino acid sequence VNITIKQHTVTTTT corresponding to the second helical region of Prion, PrP 180–193, has been shown to form amyloid aggregates in water and to possess a copper-mediated toxicity to neurons. In the present work, the interaction of PrP 180–193 and its N-terminally acetylated and C-terminally amidated derivative with model membranes formed by dipalmitoylphosphatidylcholine (DPPC) was predicted by thermodynamic models and studied by differential scanning calorimetry (DSC). Thermodynamic predictions give negative values of ΔG only when the peptides transfer, in a structured form, from water to the interface region of the DPPC membrane. The DSC peaks referring to samples prepared according to two different protocols evidence remarkable differences. When the peptides are simply added to an aqueous suspension of the DPPC membrane only the blocked peptide inserts spontaneously; on the other hand when the segments are forced to insert into the membrane, by mixing lipids and peptides during the preparation of the membrane, a different behaviour is evidenced depending on the presence or absence of free charges at the ends of peptides. Our findings suggest a topological situation in which the hydrophobic part of the two peptides inserts into the membrane at a different depth as the copper effect on the complex membrane–peptide system clearly shows. These findings might have intriguing implications on the understanding of the molecular reasons for the neurotoxicity of this prion fragment.

Introduction

Prion diseases constitute a heterogeneous group of sporadic, inheritable and transmissible neurodegenerative disorders affecting humans and a variety of other animals. They include scrapie of sheep and goats, bovine spongiform encephalopathy (BSE) and several human diseases such as Creutzfeldt–Jakob disease, Gerstmann–Straussler–Scheinker Syndrome (GSS) and familial fatal insomnia (FFI).[1,2] Transmissible spongiform encephalopathies have attracted in the last few years enormous scientific attention because they exemplify a novel mechanism of biological information transfer based on the transmission of protein conformation rather than on the inheritance of nucleic acid sequences.[3] According to this "protein only hypothesis", first outlined in general terms by Griffith[4] and updated in its final form by Prusiner[5,6] the infectious agent is a conformational isoform of PrP^c,[5] a protein normally found predominantly on the outer surface of neurons.[7–9] Introduction of the abnormal Prion conformer (PrP^{sc}) into the healthy organism would result in the pathological conversion $PrP^c \rightarrow PrP^{sc}$. The conversion of PrP^c into PrP^{sc} occurs *via* a post-translational process without any chemical modifications to the protein molecule.[10,11] However, the two proteins have very different physical properties. PrP^c has a predominantly α-helical structure, is monomeric and readily digested by proteinase K, whereas PrP^{sc} forms highly insoluble aggregates, has a large β-sheet structure content and shows a high resistance to proteolytic digestion.[12,13]

There is substantial evidence that the conversion of PrP^c into PrP^{sc} is a key molecular event in the pathogenesis of Prion diseases, but the details of the molecular mechanism involving this remarkable conformational change are poorly understood. The normal cellular form of the Prion protein is associated with the plasma membrane *via* a glycosyl-phosphatidylinositol (GPI) anchor[14] and a second transmembrane form of two topologies (N- or C-terminus in the endoplasmic reticulum lumen), is associated with the plasma membrane *via* a common transmembrane segment comprising residues 113–135.[15–17] Together with several experimental observations, this strongly supports the hypothesis that an abnormal interaction of PrP with the lipid membrane might be involved in the process of conversion of PrP^c to PrP^{sc}.[18] Unfortunately, studies on the structure of PrP^{sc} conformers and their domains involved in the lipid-assisted conformational change $PrP^c \rightarrow PrP^{sc}$ have been severely limited by the high insolubility of these molecules. Thus, to gain insights into this issue, *in vivo* and *in vitro* studies have been carried out using synthetic segments of PrP corresponding to regions of putative α-helical structure as

deduced by structural predictions[19,20] and monitoring their physico-chemical properties[21] and their cytotoxicity in primary neuronal cultures.[22] In particular, a peptide corresponding to the second helical region of the human Prion protein (VNITIKQHTVTTTT), PrP 180–193, has been shown to form amyloid fibrils and to possess a Cu(II)-mediated neurotoxicity.[22] The whole picture of these observations suggests that the PrP region including residues 180–193 might be a suitable model for the investigation of the molecular reasons for the neurotoxicity of PrP segments and peptide-induced pertubation of the cell membrane.

In general, the thermotropic phase behavior of model lipid membrane systems is highly affected by incorporation of peptides, thus providing a useful method to depict the nature of the interactions between these two classes of membrane constituents.[23] In spite of the fact that DSC is probably the most convenient and sensitive method providing information about the thermally-induced gel–liquid crystal phase transitions of lipid bilayers, very few DSC data concerning the interaction of Prion segments with lipid membranes are available in the literature.[24] In the present paper, DSC experiments have been carried out in order to investigate the possible interactions of the "free" peptide PrP 180–193 (L_1) and its "blocked" derivative N-terminally acylated/C-terminally amidated (L_2), with DPPC model membranes.

The thermotropic behaviour of the model membrane/PrP 180–193 systems has also been investigated comparatively *versus* different preparation protocols for the peptide–lipid complex. The evaluation of the experimental results in the light of thermodynamic predictions based on the models available in the literature suggests the formation of aggregated forms of the peptide in the membrane and underlines the specific role of the electrostatic interactions and of copper in modulating the lipid/peptide interactions.

Experimental

Chemicals

Peptide coupling reagents and peptide synthesis resins were purchased from Applied Byosystems. Amino acids were purchased form NovaBiochem.

1,2-Dipalmitoyl-*sn*-glycero-3-phosphocholine (DPPC) was obtained from FLUKA. All inorganic salts for phosphate buffer preparation were purchased from SIGMA Chemical Co.

Peptide synthesis

The peptide PrP 180-193 (L_1), and its N-terminally acetylated/C-terminally amidated derivative (L_2), were synthesized as reported elsewhere[25] and as briefly summarized here. A 431-A Applied Biosystem instrument was used. Fmoc-synthesized peptides were cleaved from the solid support, a resin Rink Amide MBHA from NovaBiochem (CH), using a trifluoroacetic acid (TFA)/water/triethylsilane (95:2.5:2.5) mixture over the course of 3 hours. All crude peptides were precipitated by concentration of the acid solution, resolubilized by a minimal quantity of TFA and then recrystallized many times from a methanol/ether mixture and, finally, dissolved in water and lyophilized. Purity was greater than 95% for all the peptides that were used.

Metal-depleted buffer preparation

Chelex 100-treated phosphate buffer solutions (10 mM) were prepared by suspending chelex 100 resin (50% V/V) in 50 ml of phosphate buffer and stirring for 24 hours as previously described.[26]

Preparation of large unilamellar vesicles (LUV)

Model membranes were prepared as described elsewhere.[24] Briefly, solutions of pure phospholipids in $CHCl_3$ were dried under nitrogen and evaporated under high vacuum to dryness in round-bottomed flasks. The resulting lipid film on the wall of the flask was hydrated with an appropriate volume of metal-depleted buffer and dispersed by vigorous stirring in a water bath set at 4 °C above the gel-liquid crystal transition temperature of the membrane. The final nominal concentration of the lipid was 2 mg ml^{-1}. In order to obtain large unilamellar vesicles (LUV), the multilamellar vesicles so obtained were extruded through polycarbonate filters (pore size = 100 nm) (Nuclepore, Pleasanton, CA) mounted in a mini-extruder (Avestin Inc.) fitted with two 0.5 ml Hamilton gastight syringes (Hamilton, Reno, NV). Usually we subjected samples to 19 passes through two filters in tandem as recommended elsewhere.[27] An odd number of passages was performed to avoid contamination of the sample by vesicles which might not have passed through the filter.

Incorporation of peptide segments in model membranes

Two different protocols were applied to prepare mixed lipid/peptide bilayers:

1) the peptide fragment was dissolved in the same organic solution ($CHCl_3$) of the phospholipid (molar ratio peptide/lipid of 1/10), and extruded according to the procedure described above.

2) the required amount of peptide was added to previously prepared DPPC LUVs suspensions to give a final peptide/lipid molar ratio of 1/10. The mixture was initially vigorously vortexed for 1–2 minutes and immediately scanned.

Differential scanning calorimetry

DSC scans were carried out with a second generation high-sensitivity SETARAM micro differential scanning calorimeter (microDSC III) with 1 ml stainless steel sample cells, interfaced with a BULL 200 Micral computer. The sampling rate was 1 point per second in all measuring ranges. The same solution without the sample was used in the reference (control) cell. Both the sample and reference were heated with a precision of 0.05 °C at a scanning rate of 0.5 °C min^{-1}. In order to obtain the excess heat capacity (Cp_{exc}) curves, buffer–buffer base lines were recorded at the same scanning rate and then subtracted from the sample as previously described.[24] The average level of noise was about ±0.4 μW and the reproducibility at refilling was about 0.1 mJ K^{-1} ml^{-1}. Calibration in energy was obtained by giving a definite power supply, electrically generated by an EJ2 SETARAM Joule calibrator within the sample cell. To check the reproducibility of the results, three different samples were scanned. For each sample, three heating and two cooling scans were recorded. Cooling scans yielded curves very similar to the heating scans, but, and according to the literature,[28] the transitions in cooling curves are shifted, by about 1 °C, to lower temperatures. Therefore, due to the supercooling phenomenon, accurate thermotropic transitions are generally evaluated from heating curves. For this reason, only heating scans are discussed in the present work. In the case of DPPC model membranes only the main transition is considered because the pre-transition is strongly dependent on the preparation method of the membrane and it disappears when the liposomes are extruded.[29] All DSC experiments were repeated after 24 and 48 hours, but kinetic effects were never evidenced.

Table 1 Thermodynamic parameters of coil–helix transition expressed as $\Delta G/RT$ calculated as reported in ref. 30 for L_1 at 25 °C[a]

		$N_h = 4$	$N_h = 5$	$N_h = 6$	$N_h = 7$	$N_h = 8$	$N_h = 9$	$N_h = 10$	$N_h = 11$	$N_h = 12$	$N_h = 13$	$N_h = 14$
Val 180	$N_s = 1$	0.836	0.958	1.307	1.437	1.142	1.069	0.901	1.083	1.160	0.938	1.015
Asn 181	$N_s = 2$	0.821	1.170	1.661	1.364	1.292	1.124	1.306	1.383	1.160	1.237	—
Ile 182	$N_s = 3$	0.318	0.809	1.541	1.472	1.305	1.487	1.564	1.341	1.418	—	—
Thr 183	$N_s = 4$	1.005	1.741	**2.155**	1.987	**2.169**	**2.246**	**2.024**	**2.101**	—	—	—
Ile 184	$N_s = 5$	1.233	1.647	1.857	**2.039**	**2.116**	1.894	1.971	—	—	—	—
Lys 185	$N_s = 6$	1.723	1.933	**2.335**	**2.412**	**2.189**	**2.266**	—	—	—	—	—
Gln 186	$N_s = 7$	1.646	**2.047**	**2.485**	**2.262**	**2.339**	—	—	—	—	—	—
His 187	$N_s = 8$	1.388	1.825	**2.430**	**2.507**	—	—	—	—	—	—	—
Thr 188	$N_s = 9$	1.283	1.887	**0.325**	—	—	—	—	—	—	—	—
Val 189	$N_s = 10$	1.450	1.887	—	—	—	—	—	—	—	—	—
Thr 190	$N_s = 11$	1.750	—	—	—	—	—	—	—	—	—	—

[a] N_s, helix starting residues; N_h, helix length.

Results and discussion

Thermodynamic models of lipid–peptide interactions

The driving force of the incorporation of a peptide into the lipid bilayer is generally dominated by the unfavourable free energy cost of inserting the peptide bonds into the hydrocarbon core (5 kJ mol^{-1} per peptide bond). However, if the peptide in the lipid matrix adopts a structure forming H-bonds, it can reduce this high free energy cost; thus the formation of α-helices or β-sheets can promote the incorporation of a peptide in a hydrocarbon environment. Although the primary driving force for peptide insertion into membranes arises from the free energy reduction associated with the H-bonding consequent to the increase in secondary structure content, other effects also contribute significantly, including the effects of folding/assembly entropy, side-chain packing and the relative exposure of side-chains to membrane and water. All these factors are strictly related to the hydrophobic/hydrophilic pattern of the peptide sequence. In this light, several authors have proposed a generalized model allowing a first-order prediction of the energetics of peptide–bilayer interactions based only on the peptide sequence and on its secondary structure content. All the details about these thermodynamic models have been recently reviewed.[30]

According to this point of view, the hydrophilic domains of the peptide with the lowest propensity to interact with the membranes, should also exhibit a low propensity to form an α-helix. These peptidic regions are therefore good candidates to lie on the external surface of the membrane. Thus, detailed knowledge of the energetics of peptide folding is an essential prerequisite for the subsequent study of its interaction with the membranes. The model proposed by Zhu *et al.*[31] represents an effective tool to predict the intrinsic folding potential of a peptide in water due to its propensity to form α-helices of known location and length. The application of this method to free PrP 180–193 (L_1) produced a map (see Table 1) describing the energetics of the hypothetical coil–helix transitions of the peptide relative to all the possible α-helices. Only positive values are obtained confirming that this fragment in water adopts predominantly a random coil conformation also in agreement with literature CD data.[22] In Table 1 the highest $\Delta G/RT$ values are marked in bold in order to evidence the specific peptide regions with the lowest propensity to form structured forms. It is noteworthy that this region corresponds to the most hydrophilic domain of the fragment KQH calculated according to the Kyte and Doolittle hydrophobicity scale,[32] including Hys187.

On the basis of these considerations, and applying the thermodynamic formalism proposed by White and Wimley[30] we have calculated the free energy of transfer of L_1, L_2 from water to the interface or hydrophobic core of the membrane.

The calculations were carried out assuming a random coil situation of the segments in water and two different alternative situations in membrane: structured or not structured. The calculated values reported in Table 2 show that insertion of the peptides into the hydrophobic core of the membrane is disfavoured as evidenced by the positive values of the transfer free energies, whilst insertion in the interface zone is possible only if both peptides adopt a structured form.

It can be noted that the highly hydrophobic character of L_2 with respect to L_1 is still the major driving force in controlling the lipid/peptide interaction as evidenced by the negative values of ΔG.

Experimental DSC results support these expectations and add further details to the peptide/membrane topology issue. In principle, the analysis of the heat capacity changes upon the main transition of lipid/peptide systems can help to clarify not only the effects of the presence of the peptide on the physical state of the membrane, but also the topological arrangement of the peptide when it is inserted into the lipid matrix. In fact, the enthalpy change observed during the lipid main transition is mainly ascribable to the increase in rotameric degrees of freedom for each C–C bond of the hydrocarbon tails[33] to which can be associated an energy gain of about 1 kJ mol^{-1}.[34] Thus it is possible to relate the decrease of the transition enthalpy of the bilayer with the extent of the interaction between the host molecules and hydrophobic tails of lipid membranes. Moreover, thermal studies carried out on lipids with identical hydrocarbon tails but different head groups evidenced that while the enthalpy of the transition depends mainly on the length of the tails, the transition temperature is more sensitive to the interactions that involve the head groups: in particular it has been shown that T_m increases with the rigidity of the membrane.[24,34] In this light, the DSC data reported below, coupled with the predictions of the thermodynamic models previously discussed, have allowed us to describe both energetically and topologically the interaction of PrP 180–193 segments with DPPC membranes.

Table 2 Transfer ΔG^{tr} of PrP 180–193 (L_1) and of its N-acetylated, C-amidated derivative (L_2) from water to a DPPC membrane, interface or hydrophobic core, calculated according to the model proposed in ref. 29

Peptide	Assumed form in membrane	ΔG^{tr}/kcal mol^{-1} (Water → interface)	ΔG^{tr}/kcal mol^{-1} (Water → hydrophobic core)
L_1	Unstructured	2.65	13.65
L_1	Structured	−2.95	8.05
L_2	Unstructured	0.85	7.75
L_2	Structured	−4.75	2.15

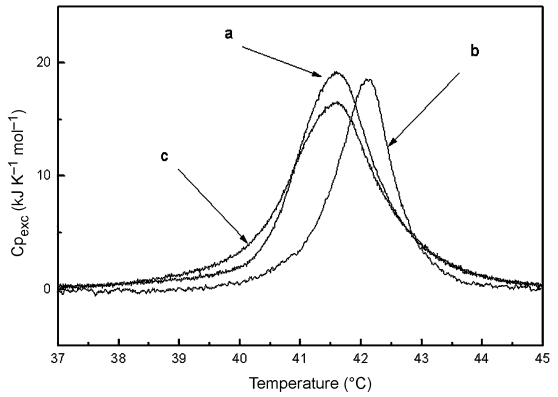

Fig. 1 DSC curves for mixtures of PrP 180–193 (L_1)/DPPC (peptide/lipid molar ratio 1:10) large unilamellar vesicles prepared according to methods 1 (curve b) and 2 (curve c). Curve a) represent the DSC transition of a pure model membrane prepared according to the same protocol. The heating rate was 0.5 K min^{-1}. All the samples were prepared in metal-depleted phosphate buffer, 10 mM, pH = 7.0; ionic strength was adjusted to 0.1 M by sodium chloride.

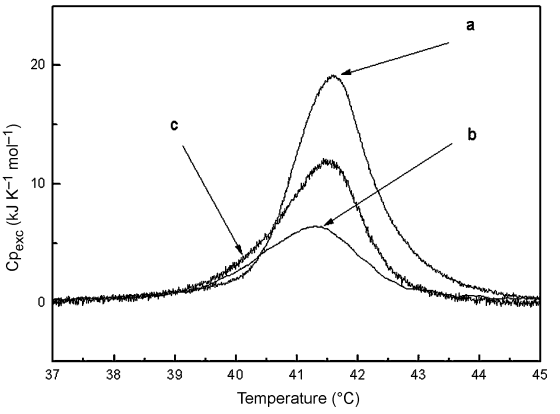

Fig. 2 DSC curves for mixtures of PrP 180–193 (L_2)/DPPC (peptide/lipid molar ratio 1:10) large unilamellar vesicles prepared according to methods 1 (curve b) and 2 (curve c). Curve a) represent the DSC transition of a pure model membrane prepared according to the same protocol. Experimental conditions are the same used for PrP 180–193 (L1)/DPPC systems.

DSC of DPPC/(L_1) systems

Fig. 1 shows the heat capacity (*C*p) profile of LUVs of pure DPPC (curve a), of DPPC/L_1 systems prepared according to method 1 (curve b) and method 2 (curve c) as reported in the experimental section. In Table 3 all the DSC parameters are reported.

A comparison of the three calorimetric profiles shows that the thermally-induced transition is differently affected by the presence of L_1 in the lipid bilayer depending on the preparation method. In particular when the host peptide is "forced" to be incorporated into the membrane (preparation method 1), the DSC peak corresponding to the thermally-induced main transition of the membrane is sharpened and shifted to higher temperatures. In particular T_m increases by about 0.5 °C and ΔH decreases by about 11 kJ mol^{-1} with respect to the corresponding values of the pure DPPC LUVs. According to standard interpretations of DSC profiles of similar systems, curve b in Fig. 1 indicates an increased rigidity of the lipid–peptide complex probably due to electrostatic interactions of the hydrophilic part of the peptide with the surface of the membrane; the decrease in the transition enthalpy corresponds to the blocking of about 1/3 of the rotamers of the hydrocarbon tails of the lipids as a consequence of the partial insertion of the hydrophobic part of the peptide into the membrane. The observed increase in T_m and sharpness of the DSC peak is indicative of an increased negative curvature of the membrane surface and, in turn, of an increased size of the DPPC vesicles as a consequence of their interaction with L_1.[35,36] When the peptide is added to the external side of DPPC LUVs (preparation method 2) the DSC peak maintains approximately the same features of the pure LUV thus evidencing a negligible peptide–membrane interaction. If we consider that the thermodynamic predictions suggest a spontaneous insertion of the Prion fragment in the interface zone of the membrane, the calorimetric results seem to indicate the existence of an energetic barrier to the spontaneous insertion of the fragment in the membrane. This barrier is ascribable to the electrostatic repulsions existing between the polar surface of the membrane and the charged end groups of L_1.

DSC of DPPC/(L_2) systems

Fig. 2 shows the heat capacity (*C*p) profile of LUVs of pure DPPC (curve a), of DPPC/L_2 systems prepared according to method 1 (curve b) and to method 2 (curve c) as reported in the experimental section. A comparison between the three calorimetric profiles shows a different behaviour if compared with DPPC/free PrP 180–193 (L_1) systems.

In particular when the blocked host peptide is forced to be incorporated into the membrane (preparation method 1), the peak corresponding to the melting of the membrane undergoes a lowering either of the transition temperature or of the enthalpy and a broadening of the DSC curve. In particular T_m and ΔH decrease by about 0.3 °C and 20 kJ mol^{-1} with respect to the pure DPPC LUVs. If we consider the absence of charged end groups, this behaviour can be explained with a deeper insertion of the fragment into the membrane that causes a decrease of the packaging of lipid molecules and the blocking of more than 50% of the rotamers. When the peptide is added to the exterior of the LUV (preparation method 2) the DSC peak exhibits approximately the same transition temperature as the pure DPPC membrane but ΔH decreases by about 13 kJ mol^{-1}; this corresponds to the blocking of about 35% of the rotamers as a consequence of a partial spontaneous interaction of L_2 with the membrane. In both cases, because of the deeper insertion of the peptide into the membrane, the electrostatic interactions between the hydrophilic part of the fragment and the surface of the membrane do not take place in agreement with thermodynamic predictions (see Tables 2 and 3). The decreased ΔH and T_m and the broadening of the DSC peak as a consequence of the interaction of L_2 with DPPC vesicles indicate an induced positive curvature of the membrane surface and a decreased size of the DPPC vesicles.[35,36]

Table 3 Calorimetric data relative to the different peptide/lipid bilayer systems and to different preparation methods. Experimental values are reported as mean ± standard deviation of three repeated experiments

	DPPC		DPPC/(L_1)		DPPC/(L_2)	
Method of preparation	T_m/°C	ΔH/kJ mol^{-1}	T_m/°C	ΔH/kJ mol^{-1}	T_m/°C	ΔH/kJ mol^{-1}
1	41.61 ± 0.02	36.0 ± 1.2	42.13 ± 0.02	24.8 ± 1.2	41.31 ± 0.01	16.2 ± 1.3
2	—	—	41.58 ± 0.02	36.2 ± 1.0	41.50 ± 0.02	23.1 ± 1.1

The effect of copper on DPPC/L_1 and DPPC/L_2 systems

Taking into account the presence of a histidine residue (Hys187) in the middle of the amino acid sequence and its potential to interact with copper, we used this metal ion as a molecular probe in order to evidence a different depth of incorporation of the prion segments L_1 and L_2 to the lipid bilayer. With this aim calorimetric DSC experiments at increasing copper/peptide molar ratios for DPPC/L_1 and DPPC/L_2 systems prepared according to methods 1 and 2 were carried out. No effects were evidenced when the L_2 fragment was used. This result is congruent with the hypothesis that the fragment is inserted so deeply in the membrane that the histidine is not available to interact with the solvent and, as a consequence, with the copper ions.

In the case of DPPC/L_1 systems prepared according to method 1 a remarkable progressive effect was evidenced when copper was added at concentrations ranging from 40 to 240 μM (peptide/copper molar ratios 1:1, 1:2, 1:3, 1:4, 1:5, 1:6). In particular, after a threshold value corresponding to a peptide/copper molar ratio of 1:4, a shoulder appears at the high temperature side of the main transition. At increasing concentrations of copper, this shoulder increases progressively, while the principal peak decreases, as reported in Fig. 3. This behaviour suggests a copper-dependent mechanism that involve a phase segregation in the organization of the lipid matrix in the DPPC/L_1 system. In order to be sure that no experimental artifacts could affect these data control experiments were carried out on pure DPPC LUVs/Cu^{2+} samples with increasing copper concentrations and no changes could be evidenced in the thermotropic behavior of the pure membrane. The different effect of copper reported for the system DPPC/L_1 prepared according to method 1 and DPPC/L_2 prepared according to method 2 despite the comparable depth of peptide insertion, suggests that the metal-binding site of PrP 180–193 possibly involves the charged N-terminus of L_1, thus resembling the copper coordination of another neurotoxic Prion peptide, PrP 106–126.[26]

Conclusions

The sum of the experimental results presented here has evidenced a different mechanism of interaction between "free" (L_1) and "blocked" (L_2) PrP segments with DPPC model membranes. In particular the interaction of the free peptide L_1 with the membrane, although thermodynamically allowed, occurs only when the fragment is "forced" to be incorporated into the membrane according to preparation protocol 1. In contrast, when the complex membrane/fragment L_1 is prepared according to protocol 2 no appreciable interactions are evidenced. These results highlight the striking role of the electrostatic barrier in driving the interaction of free PrP 180–193 with the DPPC membrane. In the case of the blocked peptide L_2 the absence of free charges allows, independently from the preparation procedure, a spontaneous insertion of the fragment into the membrane. Nevertheless the different DSC profiles evidence an insertion of peptide L_2 into the membrane at a different depth compared to that for L_1. These results are in agreement with the hypothesis of a partial incorporation of the most hydrophobic region of the peptide into the lipid matrix and an interaction of the hydrophilic part of the peptide with the surface of the membrane. Moreover according to the hydrophobicity scale proposed by Kyte and Doolittle[32] the residues Lys 185, Gln 186 and His 187 are highly hydrophilic and have, according to the ΔG values reported in Table 1, a very low propensity to fold. The effect of copper on the thermotropic behaviour of these systems supports the hypothesis that when this group of residues is available to the solvent it can interact with the external environment, giving an indirect indication of the different depth of the fragment in the membrane. As the thermodynamic model of the studied systems predicts, in each case the interaction with the membrane requires the formation of structured forms of peptide segments as occurs when single segments aggregate in the membrane. Fig. 4 reports a scheme of the proposed molecular model.

Experimental results reported in the present paper might have intriguing implications for the understanding of the molecular origin of the neurotoxicity of this fragment and of the role played by the copper ions in modulating the Prion peptide-induced perturbation of the membrane. Although the relationship between amyloidogenicity and neurotoxicity remains still unclear, recent evidence indicates that large fibrils themselves may not be the toxic species in neurodegenerative diseases and that oligomeric intermediates in the pathway of fibril formation, named protofibrils, may cause toxicity.[37] To date, general determinants for amyloid formation have eluded complete identification, but the presence of side chains that can interact with divalent metals, particularly copper, have been found to contribute significantly.[38] An increasing number of systems have been shown to display this property, including Prion,[26] Aβ from Alzheimer's,[39] α-sinuclein from Parkinson's,[40] immunoglobulin light chains[41] and β2 m from dialysis-related amyloidosis.[42] Our observations indicate that copper promotes a phase segregation in the organization of the lipid matrix in the PrP 180–193/membrane system and support the hypothesis that, at least indirectly, this observed change in the thermodynamic properties of the model membrane may trigger an abnormal, and possibly pathogenic, peptide/lipid interaction.

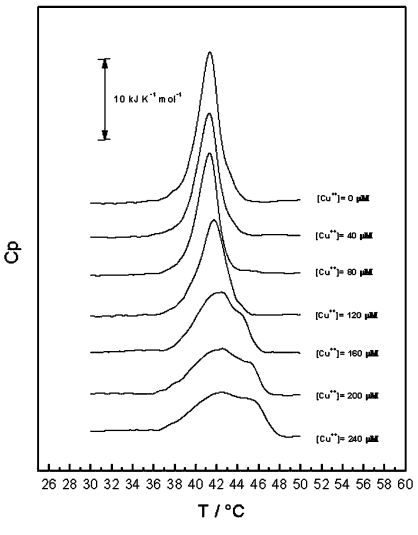

Fig. 3 DSC curves for mixtures of PrP 180–193 (L_1)/DPPC (peptide/lipid molar ratio 1:10) with increasing copper content. Experimental details are reported in the text.

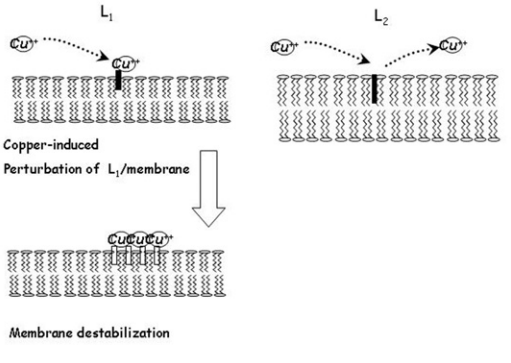

Fig. 4 Schematic models representing the possible interaction of copper with L1/DPPC and L2/DPPC membranes.

Acknowledgements

This work was partially supported by Ministero dell'Università e della Ricerca Scientifica e Tecnologica (MURST) (Grants: MM03194891, 9903032282 and 2001031717), Università degli Studi di Catania, and CNR-Agenzia 2000 Project CNR-C00781B.

References

1 D. A. Harris, *Clin. Microbiol. Rev.*, 1999, **12**, 429.
2 S. B. Prusiner, *Proc. Natl. Acad. Sci. USA*, 1998, **95**, 13 363.
3 T. Alper, W. A. Cramp, D. A. Haig and M. C. Clarke, *Nature*, 1967, **214**, 764.
4 J. S. Griffith, *Nature*, 1967, **215**, 1043.
5 S. B. Prusiner, *Annu. Rev. Microbiol.*, 1989, **43**, 345.
6 S. B. Prusiner, *Philos. Trans. R. Soc. London B: Biol. Sci.*, 1993, **339**, 239.
7 B. Oesch, D. Westaway, M. Walchli, M. P. McKinley, S. B. Kent, R. Aebersold, R. A. Bazzy, P. Tempst, D. B. Teplow, L. E. Hood, S. B. Prusiner and C. Weissmann, *Cell (Cambridge, Mass.)*, 1985, **40**, 735.
8 B. Cherebro, R. Race, K. Wahrly, J. Nischio, M. Bloom, D. Lechner, S. Bergstrom, K. Robbins, L. Mayer, J. M. Keith, C. Garon and A. Haase, *Nature*, 1985, **315**, 331.
9 K. Basler, B. Oesch, M. Walchli, D. F. Groth, M. P. McKinley, S. B. Prusiner and C. Weissmann, *Cell (Cambridge, Mass.)*, 1986, **46**, 417.
10 B. Caughey and G. J. Raymond, *J. Biol. Chem.*, 1991, **266**, 18 217.
11 N. Stahl, M. A. Boldein, D. B. Teplow, L. Hood, B. W. Gibson, A. L. Burlingame and S. B. Prusiner, *Biochemistry*, 1993, **32**, 1991.
12 B. Oesch, D. Westway, M. Walchli, M. P. McKinley, S. B. Kent, R. Aebersold, R. A. Barry, P. Tempst, D. B. Teplow and L. E. Hood, *Cell (Cambridge, Mass.)*, 1985, **40**, 735.
13 K. Pan, M. Baldwin, J. Nguyen, M. Gasset, A. Serban, D. Groth, I. Mehlhorn, Z. Huang, R. J. Fletterick, F. E. Cohen and S. B. Prusiner, *Proc. Natl. Acad. Sci. USA*, 1993, **90**, 10 962.
14 N. Stahl, D. R. Borclet, K. Hsiao and S. B. Prusiner, *Cell (Cambridge, Mass.)*, 1987, **51**, 229.
15 B. Hay, R. A. Barry, I. Llieberburg, S. B. Prusiner and V. R. Lingappa, *Mol. Cell. Biol.*, 1987, **7**, 914.
16 C. D. Lopez, C. S. Yost, S. B. Prusiner, R. M. Myers and V. R. Lingappa, *Science*, 1990, **248**, 226.
17 B. Hay, S. B. Prusiner and V. R. Lingappa, *Biochemistry*, 1987, **26**, 8110.
18 N. Sanghera and T. J. T. Pinheiro, *J. Mol. Biol.*, 2002, **315**, 1241–1256.
19 F. Lopez-Garcia, R. Zahn, R. Riek and K. Wutrich, *Proc. Natl. Acad. Sci. USA*, 2000, **97**, 8334.
20 R. Zhan, A. Liu, T. Luhrs, C. Von Schrotter, F. Lopez-Garcia, M. Billetter, L. Calzolai, G. Wider and K. Wutrich, *Proc. Natl. Acad. Sci. USA*, 2000, **97**, 145.
21 M. Gasset, M. A. Boldewin, D. H. Lloyd, J. M. Gabriel, D. M. Holtzman, F. Cohen, R. Fletterich and S. B. Prusiner, *Proc. Natl. Acad. Sci. USA*, 1992, **899**, 10 940.
22 A. Thompson, A. R. White, C. Mc Lean, C. L. Masters, R. Cappai and C. J. Barrow, *J. Neurosci. Res.*, 2000, **62**, 293.
23 *Biological Membranes*, ed. D. Chapman, Academic Press, New York, 1982, vol. 4, p. 179.
24 D. Grasso, D. Milardi, C. La Rosa and E. Rizzarelli, *New J. Chem.*, 2001, **25**, 1543.
25 V. Guantieri, G. Impellizzeri, G. Pappalardo and E. Rizzarelli, presented at XXIX Congresso Nazionale della Divisione di Chimica Inorganica della SCI, Giardini Naxos, September 2001, CT, Italy.
26 M. F. Jobling, X. Huang, L. R. Stewart, K. J. Barnham, C. Curtain, I. Volitakis, M. Perugini, A. R. White, R. A. Cheny, C. L. Masters, C. L. Barrow, S. J. Collins, A. I. Bush and R. Cappai, *Biochemistry*, 2001, **40**, 8073.
27 R. C. MacDonald, R. I. MacDonald, Ph. M. Menco, K. Takeshita, N. K. Subarrao and L. Hu, *Biochim. Biophys. Acta*, 1991, **1061**, 297.
28 M. C. Antunes-Madeira, R. A. Videira and V. M. Madeira, *Biochim. Biophys. Acta*, 1994, **1190**, 149.
29 T. Heimburg, *Biochim. Biophys. Acta*, 1998, **1415**, 147.
30 S. H. White and W. C. Wimley, *Annu. Rev. Biophys. Biomol. Struct.*, 1999, **28**, 319.
31 Y. Zhu, C. C. Chen, J. A. King and L. B. Evans, *Biochemistry*, 1992, **31**, 10 591.
32 J. Kyte and R. F. Doolittle, *J. Mol. Biol.*, 1982, **157**, 105.
33 J. F. Nagle, *Annu. Rev. Phys. Chem.*, 1980, **31**, 175.
34 P. J. Flory, *Science*, 1975, **188**, 1268.
35 K. Matsuzaki, K. Sugishita, N. Ishibe, M. Ueha, S. Nakata, K. Miyajima and R. M. Epand, *Biochemistry*, 1998, **37**, 11 856.
36 T. Brumm, K. Jorgensen, O. G. Mouritsen and T. M. Bayerl, *Biophys. J.*, 1996, **70**, 1373.
37 M. Anguiano, R. J. Nowak and P. T. Lansbury, *Biochemistry*, 2002, **41**, 11 338.
38 C. M. Eakin, J. D. Knight, C. M. Morgan, M. A. Gelfand and A. D. Miranker, *Biochemistry*, 2002, **41**, 10 646.
39 T. Miura, K. Suzuki, N. Kohata and K. Takeuchi, *Biochemistry*, 2000, **39**, 7024.
40 V. N. Uversky, J. Li and A. L. Fink, *J. Biol. Chem.*, 2001, **276**, 44 284.
41 D. P. Davis, G. Gallo, S. M. Vogen, J. L. Dul, K. L. Sciarretta, A. Kumar, R. Raffen, F. J. Stevens and Y. Argon, *J. Mol. Biol.*, 2001, **313**, 1021.
42 C. J. Morgan, M. Gelfand, C. Atreya and A. D. Miranker, *J. Mol. Biol.*, 2001, **309**, 339.